

Single file to ballistic transport phase transition in a 1d driven tracer model

Asaf Miron¹, David Mukamel¹ and Harald A Posch²

¹*Department of Physics of Complex Systems, Weizmann Institute of Science, Rehovot 7610001, Israel and*

²*Computational Physics Group, Faculty of Physics, University of Vienna, Austria*

The effect of particle overtaking on transport in a narrow channel is studied using a 1d model of a driven tracer in a quiescent bath. In contrast with the well-studied non-driven case, where the tracer's long-time dynamics is diffusive whenever overtaking is allowed, the driven tracer is shown to retain the hallmark single-file, sub-diffusive behavior for finite overtaking rates. Beyond a critical rate, the model exhibits a non-equilibrium phase transition from single-file to ballistic transport. The tracer velocity and the bath density profile are studied in both the single file and ballistic phases, demonstrating the distinct features of these phases.

The motion of a tracer (tagged particle) in a bath of similar particles confined to a narrow channel is a classical problem which has attracted a wealth of theoretical and experimental studies for several decades. For a sufficiently narrow channel, where particles cannot overtake each other, the motion of the tracer, known as single file (SF) diffusion, is rather constrained due to strong spatial and temporal correlations between particles, which are generated by the geometrical confinement. As a result, for example, the mean-square displacement of a tracer grows sub-diffusively at long time as \sqrt{t} , rather than linearly as is the case in ordinary diffusion [1–3]. An interesting question is how does the motion of the tracer change from SF to ordinary diffusion when the channel becomes wide enough to allow particle overtaking. Many studies devoted to this question have shown that the crossover from SF sub-diffusion to ordinary diffusion is smooth, with diffusion dominating at asymptotically long times for any finite overtaking rate [4–7]. This crossover can be described by a time dependent "diffusion constant" $\langle x^2 \rangle \propto D(t)t$. At short times $D(t) \propto 1/\sqrt{t}$ yields SF behavior whereas at long times $D(t)$ approaches a non-vanishing constant, as expected in ordinary diffusion.

New developments in experimental techniques, such as microreohology [8] and microfluidics [9], make it possible to locally manipulate fluids of interacting particles, either by optical or magnetic means [10, 11]. These experimental tools have been used in many studies of complex fluids with constrained dynamics such as polymer solutions [12–14], colloids [15, 16], granular systems [17] and others [18–20]. On the theoretical side, this has led to numerous studies of various models in which a *driven tracer* moves in a narrow channel of quiescent medium [21–27]. In the absence of overtaking, SF sub-diffusion is similarly observed in the driven case, with the mean square displacement growing as \sqrt{t} at large t . On an infinitely-long system the tracer position, too, grows as \sqrt{t} [21–23, 26, 28], while for a finite system, say, a ring of length L , a finite steady state velocity $v \sim \mathcal{O}(L^{-1})$

is maintained [26, 29]. A natural open question is, how does the motion of a driven tracer change when overtaking with the bath particles is allowed. In particular, can the SF behavior be maintained at small overtaking rates or does it asymptotically cross over to ordinary diffusion, as in the non-driven case.

In this letter we address this question by considering a 1d driven tracer model and studying its behavior in the presence of overtaking. Using mean-field (MF) analysis, together with numerical simulations, we demonstrate that unlike the smooth crossover observed in equilibrium, non-driven settings, the SF behavior in this model persists for small but finite overtaking rates. It changes to ballistic behavior via a phase transition which occurs at some finite overtaking rate. In the limit of large system size, L , the SF phase is characterized by sub-diffusive tracer dynamics and an average tracer velocity which scales as $v \sim L^{-1}$. The corresponding bath density profile, which is stationary in the tracer reference frame, is macroscopic and extends throughout the entire system. On the other hand, in the ballistic phase the average velocity v is finite, the mean square displacement of the tracer grows linearly with time, and the density profile is localized around the tracer.

The model: We consider a 1d ring of L sites labeled by $\ell = 0, 1, \dots, L-1$, occupied by one tracer particle and N bath particles whose density is denoted by $\bar{\rho} = \frac{N}{L-1}$. The particles interact through simple exclusion whereby each site holds one particle at most. The bath particles evolve by symmetric simple exclusion process (SSEP) dynamics. They attempt to hop to neighboring right or left sites with equal rates 1 whereas the tracer hopping rates are p to the right and q to the left. Hops only occur if the target site is vacant. In addition, the tracer tries to exchange places with a bath particle occupying the neighboring right site with rate p' and the left site with rate q' , if a bath particle is present at these sites. These dynamics are illustrated by

$$10 \xleftrightarrow{1} 01 \quad ; \quad 20 \xleftrightarrow[q]{p} 02 \quad ; \quad 21 \xleftrightarrow[q']{p'} 12$$

where vacant sites, bath particles and the tracer are respectively denoted by 0, 1 and 2 and the rates of each process are depicted by the corresponding arrows.

The case of vanishing exchange rates $p' = q' = 0$, which corresponds to SF dynamics has been extensively studied in the past. Here we are interested in the effect of exchange processes on the steady state of the model. In particular we evaluate the steady state properties of the model in the reference frame of the tracer, located at site $\ell = 0$. It is worthwhile noting the following symmetry properties of the model. Under space inversion $\ell \rightarrow L - \ell$ together with rates exchange $p \leftrightarrow q$ and $p' \leftrightarrow q'$ the steady state density profile in the tracer's frame transforms as $\rho_\ell \rightarrow \rho_{L-\ell}$ together with velocity reversal of the tracer $v \rightarrow -v$. Another transformation is particle-hole exchange (which leads to $\bar{\rho} \rightarrow 1 - \bar{\rho}$) together with $p \leftrightarrow p'$ and $q \leftrightarrow q'$. Here the steady state density profile transforms as $\rho_\ell \rightarrow 1 - \rho_\ell$ and the tracer's velocity stays unchanged.

Main Results: Before presenting our analysis, we briefly summarize the main results obtained by MF calculations and numerical simulations. These demonstrate the existence of a phase transition separating a SF phase, with $v \propto 1/L$ and sub-diffusive tracer dynamics, from a ballistic phase, with finite v and diffusive dynamics. The results are most conveniently presented when the hop and exchange rates are rewritten as

$$\begin{cases} p = r(1 + \delta) ; q = r(1 - \delta) \\ p' = r'(1 + \delta') ; q' = r'(1 - \delta') \end{cases}, \quad (1)$$

where r and r' are the average hopping and exchange rates, respectively, while $r\delta$ and $r'\delta'$ are the biases in these rates. Here $r, r' \geq 0$ and $-1 \leq \delta, \delta' \leq 1$. In the MF analysis we find two critical manifolds at average densities $\bar{\rho}_c^I$ and $\bar{\rho}_c^{II}$ given by

$$\bar{\rho}_c^I = \delta(1 - \delta') / (\delta - \delta') ; \bar{\rho}_c^{II} = \delta(1 + \delta') / (\delta - \delta'). \quad (2)$$

Note that the two manifolds are independent of the average rates r and r' and thus the phase diagram can be represented in the three-dimensional parameter space $\{\bar{\rho}, \delta, \delta'\}$. For convenience and without loss of generality, we take $\delta > 0$ in the rest of the paper.

The SF phase exists for $\delta' < 0$ at average density $\bar{\rho}_c^I < \bar{\rho} < \bar{\rho}_c^{II}$. Outside this range, namely at low ($\bar{\rho} < \bar{\rho}_c^I$), and high ($\bar{\rho} > \bar{\rho}_c^{II}$) average density, the phase is ballistic. A typical phase diagram in the $(\delta', \bar{\rho})$ plane is depicted in Fig. 1. A different section, in the (δ, δ') plane, is presented in the supplemental material.

The phase diagram and the nature of the phase transition may be understood as follows: At low density, there are few bath particles behind the tracer with which it can exchange places. Consequently, hopping domi-

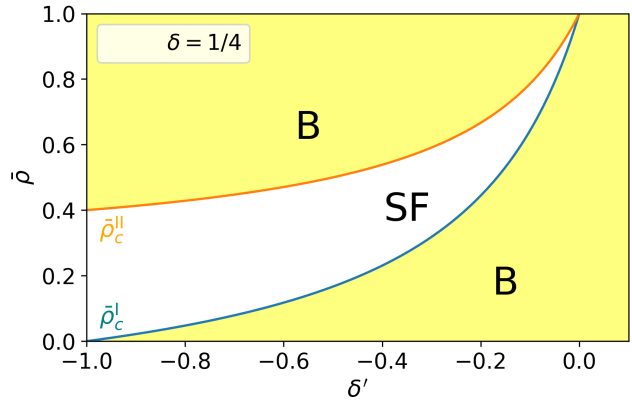


Figure 1. The phase diagram in the $(\delta', \bar{\rho})$ plane for fixed $\delta = 1/4$, indicating the transition lines between the ballistic (B) and single file (SF) phases.

nates over exchange. Since $\delta > 0$, a positive steady-state tracer velocity $v > 0$ arises, indicating that the system is in the ballistic phase. In this phase the moving tracer generates, in its reference frame, a stationary bath-particle density profile with some induced density excess localized ahead of the tracer. The extent of this region and the number of bath particles entrained in it are of $\mathcal{O}(1)$ compared with N and L , respectively. As the average density increases, more bath particles are found near the tracer, making the exchange process more pronounced. For $\delta' < 0$, particles are effectively "pumped" from behind the tracer, increasing the density excess region ahead. At the critical density $\bar{\rho} = \bar{\rho}_c^I$ this region becomes macroscopically large of $\mathcal{O}(L)$, the tracer's velocity vanishes and a transition to the SF phase takes place. The transition is continuous in the tracer's velocity, which vanishes when approaching the transition from the ballistic phase as

$$v = s(\bar{\rho}_c^I - \bar{\rho}), \quad (3)$$

with s a constant given in Eq. (16).

To establish this picture, Fig. 2 shows the steady-state tracer velocity against $\bar{\rho}$ for given hopping and exchange rates, as obtained by MF calculations and numerical simulations. At low density, the system is in the ballistic phase and the tracer velocity is finite and positive due to the hopping bias $p > q$. When $\bar{\rho}$ crosses $\bar{\rho}_c^I$, the system enters the SF phase where v becomes vanishingly small as $1/L$ for large L . Particle-hole symmetry yields a similar picture as $\bar{\rho}$ grows past $\bar{\rho}_c^{II}$, leading the system back into the ballistic phase, this time with $v < 0$ driven by the exchange bias $q' > p'$.

In the SF phase, the mean square displacement of the tracer's position exhibits sub-diffusive scaling, similar to

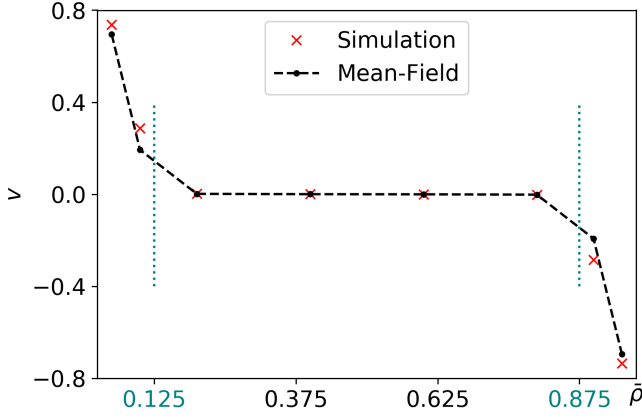


Figure 2. The tracer velocity v versus the bath density $\bar{\rho}$ as obtained from MF analysis and numerical simulations for $L = 4096$ and rates $p = q' = 1.75$, $q = p' = 0.25$. The vertical dotted (teal) lines indicate the critical values predicted by MF (Eq. (2)). The dashed line serves as a guide for the eye.

the typical sub-diffusive behavior observed in SF models [21–23, 26, 28], as demonstrated numerically in the supplemental material.

In Fig. 3 we present the density profile in the tracer's frame. Panel A shows a collapse as a function of $x = \ell/L$ in the SF phase, where the $\sim \mathcal{O}(L)$ density excess ahead of the tracer is macroscopically large and extends throughout the system. Panels B and C show a collapse as a function of ℓ in the ballistic phase. Here, the $\sim \mathcal{O}(1)$ density excess is localized, leaving the density in the rest of the system basically unchanged $\approx \bar{\rho}$. The excellent agreement in Figs. 2 and 3 between the numerical simulation results and the MF calculations suggests that the model's stationary behavior is well approximated by the MF description.

MF Analysis: We next compute the stationary properties of the model in the MF approximation, where correlations between the occupation of different sites are neglected, focusing on the bath density profile and average tracer velocity. To this end, we first formulate the MF equations for the bath density ρ_ℓ at sites $\ell = 1, 2, \dots, L-1$ in the tracer's reference frame, whose position is set to $\ell = 0$. The equation for ρ_ℓ in the bulk of the system, i.e. at sites $\ell \in [2, L-2]$, is

$$\partial_t \rho_\ell = \rho_{\ell+1} - 2\rho_\ell + \rho_{\ell-1} + v_+ (\rho_{\ell+1} - \rho_\ell) - v_- (\rho_\ell - \rho_{\ell-1}) \quad (4)$$

whereas, at the first and last sites $\ell = 1$ and $\ell = L-1$,

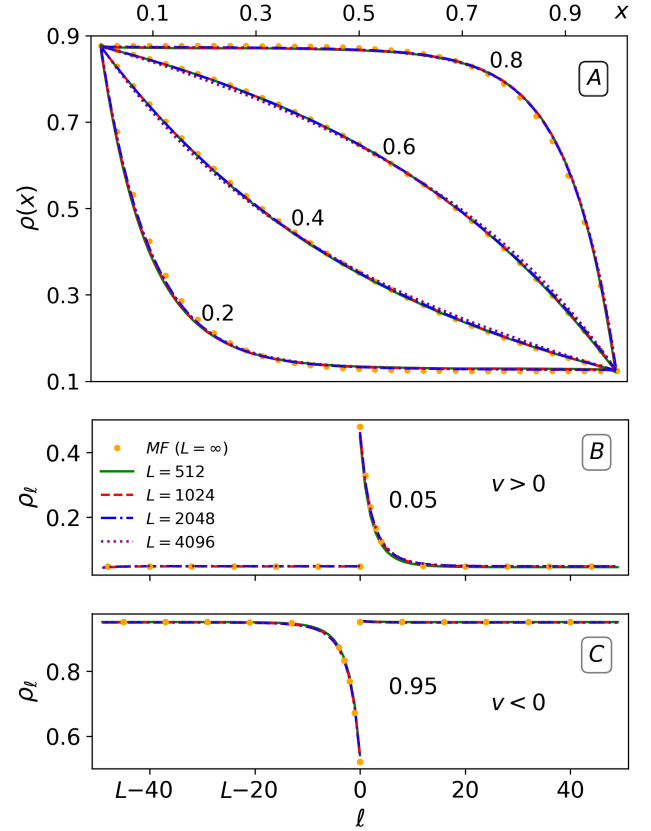


Figure 3. Density profile collapse with respect to L for different values of $\bar{\rho}$, alongside the corresponding MF solution. The value of $\bar{\rho}$ is indicated for every curve. Each curve represents data for four values of L , as listed in the figure. Panel A describes the SF phase, where the collapse is a function of $x = \ell/L$ and the density profile extends throughout the system. Panels B and C correspond to the ballistic phase, where the density profile is localized around the tracer at $\ell = 0$. In panel B, $v > 0$ and particles accumulate to the right of the tracer while in pane C, $v < 0$ and vacancies accumulate to its left.

the density satisfies the boundary equations

$$\begin{cases} \partial_t \rho_1 = (1 - \rho_1) (\rho_2 (1 + p) + q' \rho_{L-1}) \\ -\rho_1 (1 - \rho_2) (1 + p') - q (1 - \rho_{L-1}) \rho_1 \\ \partial_t \rho_{L-1} = (1 - \rho_{L-1}) (\rho_{L-2} (1 + q) + p' \rho_1) \\ -\rho_{L-1} (1 - \rho_{L-2}) (1 + q') - p \rho_{L-1} (1 - \rho_1). \end{cases}, \quad (5)$$

The tracer moving rates to the right v_+ and left v_- are given by

$$v_+ = p(1 - \rho_1) + p' \rho_1; \quad v_- = q(1 - \rho_{L-1}) + q' \rho_{L-1} \quad (6)$$

and are used to define the tracer velocity $v = v_+ - v_-$ and the total rates of move $u = v_+ + v_-$. The stationary

bulk equation (4) then becomes

$$0 = \rho_{\ell+1} - 2\rho_{\ell} + \rho_{\ell-1} + c(\rho_{\ell+1} - \rho_{\ell-1})/2, \quad (7)$$

where $c = v/(1 + u/2)$. The resulting density profile is

$$\rho_{\ell} = A + (\rho_1 - A) [(2 - c)/(2 + c)]^{\ell-1}, \quad (8)$$

where the parameters A , c and ρ_1 are determined by the boundary Eqs. (5) and the normalization $\sum_{\ell=1}^{L-1} \rho_{\ell} = N$. Within this framework, we separately analyze the two phases of the system by self-consistently determining the large- L dependence of the tracer velocity v in the SF and ballistic phases.

The SF Phase: The tracer velocity v in the SF phase is assumed to vanish with L as $v \sim \mathcal{O}(L^{-1})$. Taking $c \equiv a/(L - 1)$, where a is a constant, and considering the limit of large L , a continuum limit of Eq. (7) is obtained. In this limit the density profile can be written as $\rho_{\ell} = \rho^{SF}(x \equiv \ell/(L - 1))$ with $0 \leq x \leq 1$ and $\int_0^1 dx \rho^{SF}(x) = \bar{\rho}$. The scaled density function $\rho^{SF}(x)$ is given by

$$\rho^{SF}(x) = A + (\rho_1 - A)e^{-ax}, \quad (9)$$

where A and a are determined by the boundary equation

$$\rho_{L-1} = A + (\rho_1 - A)e^{-a} \quad (10)$$

and the normalization condition $\bar{\rho} = A + (\rho_1 - A)W$, where $W = (1 - e^{-a})/a$.

The densities ρ_1 and ρ_{L-1} can be determined using the boundary Eqs. (5) by noting that in the SF phase ρ_2 and ρ_{L-2} are equal to ρ_1 and ρ_{L-1} , respectively, up to negligible terms of order $\mathcal{O}(L^{-1})$. As a result, these densities are found to be

$$\rho_1^{SF} = \frac{q'(p - q)}{q'p - p'q} \quad \text{and} \quad \rho_{L-1}^{SF} = \frac{p'(p - q)}{q'p - p'q}. \quad (11)$$

When inserted into Eq. (10) and the normalization condition, these expressions determine A and provide an explicit (transcendental) equation for a ,

$$aW(\rho_1 - \bar{\rho}) = (1 - W)(\rho_1 - \rho_{L-1}). \quad (12)$$

Note that the SF phase exists only when the hopping drive $(p - q)$ and the exchange drive $(p' - q')$ have opposite signs. This simply follows from the requirement that the SF solution for the density should satisfy $0 \leq \rho_1^{SF}, \rho_{L-1}^{SF} \leq 1$.

The density profile in the SF phase can be used to determine the transition into the ballistic phase. Assume first that the tracer moves to the right with $v > 0$. A density excess is generated in an $\mathcal{O}(L)$ region ahead of the moving tracer. Within the SF phase, ρ_{L-1}^{SF} satisfies

$\rho_{L-1}^{SF} < \bar{\rho}$ since the region ahead of the tracer contains a macroscopic fraction of the bath particles. On the other hand, in the ballistic phase the density excess is localized and one has $\rho_{L-1} = \bar{\rho}$ since the bulk density is just the average density. Thus, assuming that the phase transition is continuous, as is verified numerically, the transition occurs at $\rho_{L-1}^{SF} = \bar{\rho}$. Similarly, in the case of $v < 0$ the density excess is generated behind the tracer and the transition takes place at $\rho_1^{SF} = \bar{\rho}$. Using the expressions for ρ_{L-1}^{SF} and ρ_1^{SF} in Eq. (11) we find that the transition takes place at the two manifolds given in Eq. (2).

We conclude the SF analysis by noting that, in the large a limit, Eq. (12) becomes

$$a \approx \frac{(p - q)(p' - q')}{p'(p - q) - (q'p - p'q)\bar{\rho}}. \quad (13)$$

with vanishing denominator at the transition. The divergence of a indicates the change of the large- L behavior of c from a/L in the SF phase to a finite value in the ballistic phase.

The Ballistic Phase: In the ballistic phase c does not vanish at large L and, thus, any deviation of the bath density profile ρ_{ℓ} from its mean value $\bar{\rho}$ is localized in an $\mathcal{O}(1)$ region ahead of the tracer. In particular, one has $\rho_{L-1} \approx \bar{\rho}$ if $c > 0$ and $\rho_1 \approx \bar{\rho}$ if $c < 0$, up to $\mathcal{O}(L^{-1})$ corrections. Again, we analyze the case $c > 0$. The density profile in this phase is given by Eq. (8) with $A = \bar{\rho}$. In order to determine ρ_1 and c we note that $\rho_{L-1} = \rho_{L-2} (= \bar{\rho})$, due to the exponential decay of the density profile at large distances. Using this in the boundary equation for ρ_{L-1} , one can express ρ_1 in terms of $\bar{\rho}$ and the dynamical rates of the model. This expression may in turn be used to determine c through Eq. (6).

The expressions for ρ_1 and c take simple forms near the transition. At the transition, where $c = 0$, the density profile coincides with that of the SF phase, where

$$\rho_1 \equiv \rho_{1c} = \frac{q'(p - q)}{q'p - p'q} \quad ; \quad \rho_{L-1} = \bar{\rho}_c = \frac{p'(p - q)}{q'p - p'q}. \quad (14)$$

At small deviations from the critical density, namely for $\bar{\rho} = \bar{\rho}_c + \delta\bar{\rho}$ and $\rho_1 = \rho_{1c} + \delta\rho_1$, the boundary equation for ρ_{L-1} becomes

$$\delta\rho_1 = \frac{p(1 - \rho_{1c}) + p'\rho_{1c} - (q - q')(1 - 2\bar{\rho}_c)}{p'(1 - \bar{\rho}_c) + p\bar{\rho}_c} \delta\bar{\rho}, \quad (15)$$

to linear order in these deviations. The velocity of the tracer, which is given by $v = -(p - p')\delta\rho_1 + (q - q')\delta\bar{\rho}$, becomes

$$v = -\frac{(p'q - q'p)^2}{pp'(p - q + q' - p')} \delta\bar{\rho} + \mathcal{O}(\delta\bar{\rho}^2). \quad (16)$$

Thus we find that in the ballistic phase the tracer's velocity grows linearly with the deviation of the average density from its critical value.

In conclusion, our study suggests that geometrically-constrained driven tracer transport exhibits a phase transition from single-file to ballistic behavior when overtaking processes are allowed. It is of interest to study the behavior of multiple tracers in this model. Preliminary studies show that tracers strongly attract each other, generating a macroscopic condensate. We leave this discussion to a forthcoming publication. It would also be interesting to study the effect of overtak-

ing on other set-ups of transport in constrained geometry, such as particles moving in a narrow channel, and test the existence of the phase transition and condensation found in the present study.

ACKNOWLEDGMENTS

We thank Julien Cividini and Oren Raz for suggestions and critical reading of the manuscript. This work was supported by a research grant from the Center of Scientific Excellence at the Weizmann Institute of Science.

-
- [1] DW Jepsen. Dynamics of a simple many-body system of hard rods. *Journal of Mathematical Physics*, 6(3):405–413, 1965.
- [2] Jerome K Percus. Anomalous self-diffusion for one-dimensional hard cores. *Physical Review A*, 9(1):557, 1974.
- [3] S Alexander and P Pincus. Diffusion of labeled particles on one-dimensional chains. *Physical Review B*, 18(4):2011, 1978.
- [4] Jimaan Sané, Johan T Padding, and Ard A Louis. The crossover from single file to fickian diffusion. *Faraday discussions*, 144:285–299, 2010.
- [5] Ullrich Siems, Christian Kreuter, Artur Erbe, Nadine Schwierz, Surajit Sengupta, Paul Leiderer, and Peter Nielaba. Non-monotonic crossover from single-file to regular diffusion in micro-channels. *Scientific reports*, 2:1015, 2012.
- [6] AV Anil Kumar. Crossover from normal diffusion to single-file diffusion of particles in a one-dimensional channel: Lj particles in zeolite zsm-22. *Molecular Physics*, 113(11):1306–1310, 2015.
- [7] Sheida Ahmadi and Richard K Bowles. Diffusion in quasi-one-dimensional channels: A small system n, p, t, transition state theory for hopping times. *The Journal of chemical physics*, 146(15):154505, 2017.
- [8] Laurence G Wilson and Wilson CK Poon. Small-world rheology: an introduction to probe-based active microrheology. *Physical Chemistry Chemical Physics*, 13(22):10617–10630, 2011.
- [9] Brian J Kirby. *Micro-and nanoscale fluid mechanics: transport in microfluidic devices*. Cambridge university press, 2010.
- [10] David G Grier. A revolution in optical manipulation. *nature*, 424(6950):810, 2003.
- [11] F Wittbracht, A Weddemann, A Auge, and A Hütten. Flow guidance of magnetic particles by dipolar particle interaction. In *2010 Fourth International Conference on Quantum, Nano and Micro Technologies*, pages 102–106. IEEE, 2010.
- [12] Christof Gutsche, Friedrich Kremer, Matthias Krüger, Markus Rauscher, Rudolf Weeber, and Jens Harting. Colloids dragged through a polymer solution: Experiment, theory, and simulation. *The Journal of chemical physics*, 129(8):084902, 2008.
- [13] Matthias Krüger and Markus Rauscher. Diffusion of a sphere in a dilute solution of polymer coils. *The Journal of chemical physics*, 131(9):094902, 2009.
- [14] Chen Wang, Xiao Zhong, David B Ruffner, Alexandra Stutt, Laura A Philips, Michael D Ward, and David G Grier. Holographic characterization of protein aggregates. *Journal of pharmaceutical sciences*, 105(3):1074–1085, 2016.
- [15] Marco Polin, Yohai Roichman, and David G Grier. Autocalibrated colloidal interaction measurements with extended optical traps. *Physical Review E*, 77(5):051401, 2008.
- [16] Roel PA Dullens and Clemens Bechinger. Shear thinning and local melting of colloidal crystals. *Physical review letters*, 107(13):138301, 2011.
- [17] Raphaël Candelier and Olivier Dauchot. Journey of an intruder through the fluidization and jamming transitions of a dense granular media. *Physical Review E*, 81(1):011304, 2010.
- [18] Julien Cividini, Anupam Kundu, Satya N Majumdar, and David Mukamel. Exact gap statistics for the random average process on a ring with a tracer. *Journal of Physics A: Mathematical and Theoretical*, 49(8):085002, 2016.
- [19] J Cividini, A Kundu, Satya N Majumdar, and D Mukamel. Correlation and fluctuation in a random average process on an infinite line with a driven tracer. *Journal of Statistical Mechanics: Theory and Experiment*, 2016(5):053212, 2016.
- [20] A Kundu and J Cividini. Exact correlations in a single-file system with a driven tracer. *EPL (Europhysics Letters)*, 115(5):54003, 2016.
- [21] SF Burlatsky, GS Oshanin, AV Mogutov, and M Moreau. Directed walk in a one-dimensional lattice gas. *Physics Letters A*, 166(3-4):230–234, 1992.
- [22] SF Burlatsky, G Oshanin, M Moreau, and WP Rein-

- hardt. Motion of a driven tracer particle in a one-dimensional symmetric lattice gas. *Physical Review E*, 54(4):3165, 1996.
- [23] J De Coninck, G Oshanin, and M Moreau. Dynamics of a driven probe molecule in a liquid monolayer. *EPL (Europhysics Letters)*, 38(7):527, 1997.
- [24] C Landim, S Olla, and SB Volchan. Driven tracer particle in one dimensional symmetric simple exclusion. *Communications in mathematical physics*, 192(2):287–307, 1998.
- [25] O Bénichou, AM Cazabat, A Lemarchand, M Moreau, and G Oshanin. Biased diffusion in a one-dimensional adsorbed monolayer. *Journal of statistical physics*, 97(1-2):351–371, 1999.
- [26] P Illien, O Bénichou, C Mejía-Monasterio, G Oshanin, and R Voituriez. Active transport in dense diffusive single-file systems. *Physical review letters*, 111(3):038102, 2013.
- [27] O Bénichou, P Illien, G Oshanin, A Sarracino, and R Voituriez. Tracer diffusion in crowded narrow channels. *Journal of Physics: Condensed Matter*, 30(44):443001, 2018.
- [28] G Oshanin, O Bénichou, SF Burlatsky, and M Moreau. Biased tracer diffusion in hard-core lattice gases: Some notes on the validity of the einstein relation. In *Instabilities and Nonequilibrium Structures IX*, pages 33–74. Springer, 2004.
- [29] Julien Cividini, David Mukamel, and HA Posch. Driven tracers in narrow channels. *Physical Review E*, 95(1):012110, 2017.

SUPPLEMENTAL MATERIAL

Here we present additional figures to supplement the results presented in the main text.

1. Phase Diagram

In Fig. 4 the (δ, δ') phase diagram for density $\bar{\rho} = 1/4$, as predicted by the MF analysis, is shown. Ballistic and SF regions are indicated.

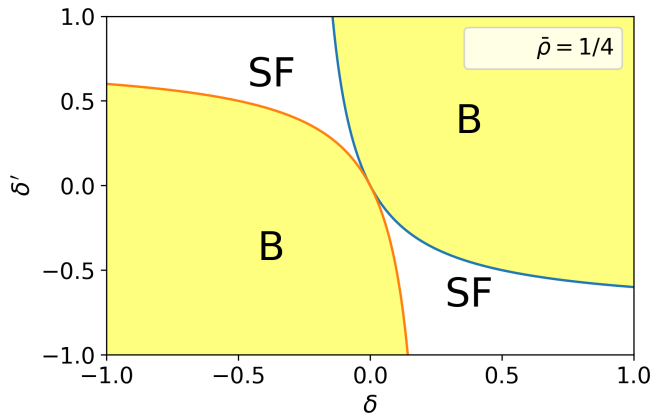


Figure 4. The phase diagram for average bath density $\bar{\rho} = 1/4$. The ballistic and single-file phases are respectively denoted by B and SF.

2. SF Phase Behavior

Figure 5 presents the long time behavior of the tracer's displacement and mean square displacement in both the SF and ballistic phases.

3. v vs L^{-1}

In Fig. 6 we plot the tracer velocity v as a function of the inverse system length $1/L$ for $\bar{\rho}$ in the ballistic and SF phases. It is evident that the velocity in the SF phase decreases as $1/L$ while in the ballistic phase it barely changes with L , approaching a non-vanishing constant at large L .

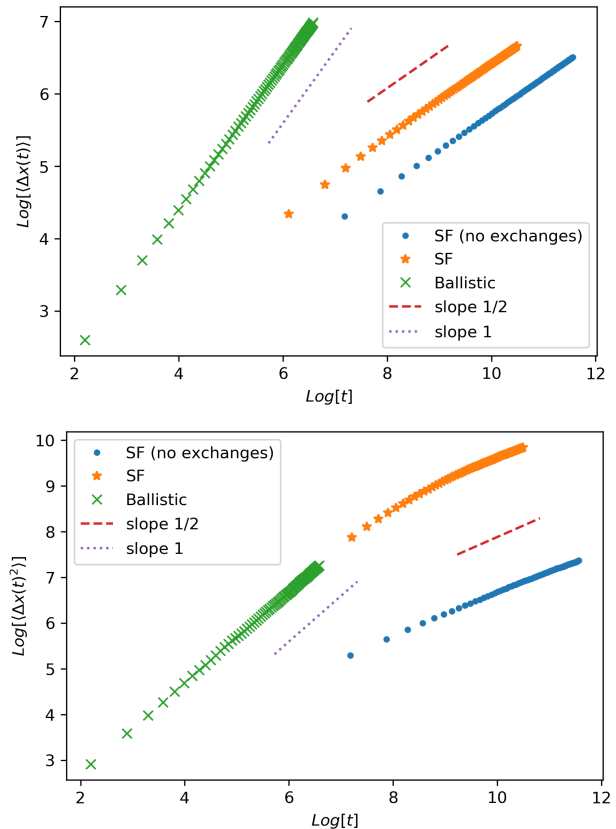


Figure 5. Temporal scaling of the tracer's mean displacement $\langle \Delta x(t) \rangle$ (top panel) and variance $\langle \Delta x^2(t) \rangle$ (bottom panel) in log-log scale for a system of $L = 4096$ sites and mean density $\bar{\rho} = 0.2$. Simulation data for the "classical" SF case without exchange dynamics, i.e. for $p' = q' = 0$, $p = 1.75$ and $q = 0.25$, is represented by blue dots. Data for the SF phase with the parameters considered in this study, $p = q' = 1.75$ and $q = p' = 0.25$, are represented by orange stars. Data for the ballistic phase, $p = p' = 1.75$ and $q = q' = 0.25$, is represented by green x's. For visual reference slope $1/2$ is presented by a red dashed line and slope 1 is presented by a purple dotted line.

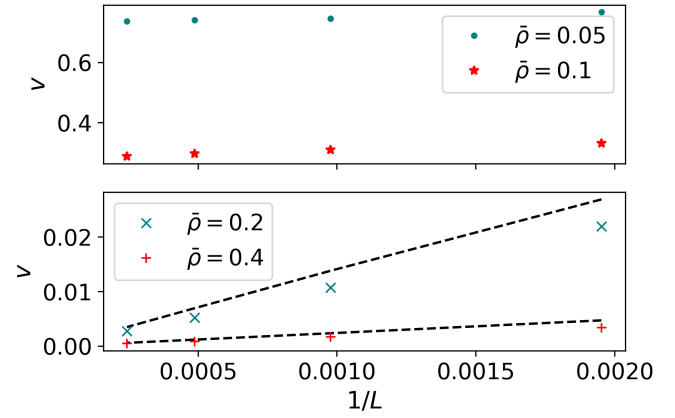


Figure 6. The tracer velocity v plotted against $1/L$ for different values of $\bar{\rho}$ in the ballistic and SF phases and for the rates $p = q' = 1.75$, $q = p' = 0.25$. Top Panel: Data in the ballistic phase, indicating that v approaches a finite constant at large L . Bottom Panel: Data in the SF phase alongside the MF solution (dashed black lines).